Industrial imaging using bremsstrahlung generated by a laser-plasma accelerator

Contact *dan.symes@stfc.ac.uk*

Matt Gear, Chris Armstrong, Gregory Hull, Stephen Dann, Daniel Symes, & Kathryn Welsby

Central Laser Facility,
STFC Rutherford Appleton Laboratory, Didcot OX11 0QX

Matthew Streeter & Gianluca Sarri

School of Mathematics and Physics,
Queen's University of Belfast, Belfast BT7 1NN

Neil Glover, Carl Boettcher, & Ellis Chong

Rolls-Royce plc. Moor Lane, Derby, PO Box 31, DE24 8BJ

Introduction

The Central Laser Facility (CLF) hosts the UK's most powerful lasers including Vulcan, Gemini and the upcoming Extreme Photonics Applications Centre (EPAC). EPAC is a new state-of-the-art high-power laser facility that is designed to drive forward scientific understanding of laser-driven accelerators, imaging sources, and to further practical applications of high-power lasers. It is expected to be operational for initial experiments in 2025 (not at full design specification) for users from across academia and industry. EPAC will be able to obtain high resolution tomographic images of a wide range of objects including complex dynamic structures, such as running engines and fluid flows.

The Gemini laser (~300 TW) has already proved capable of producing high quality images of samples [1–4], but is limited by source instability and a relatively low repetition rate (1 pulse per 20 seconds). EPAC will operate with 1 PW peak power at a 10 Hz repetition rate, providing a major increase in capability and capacity over Gemini. In contrast to previous generations of chirped pulse amplification lasers, EPAC has followed an industrial design approach benefiting from the CLF's experience in delivering commercial DiPOLE based high energy lasers to HiLASE [5] and the European XFEL [6]. Better building infrastructure, increased system monitoring, active feedback stabilisation, and machine-learning optimisation [7] will all lead to huge improvements in the performance of secondary radiation sources.

A major application for EPAC radiation sources will be high-energy x-ray imaging, particularly in the region above 300 keV, which is beyond the range of synchrotrons, commercial x-ray tubes, and compact inverse Compton scattering sources [8]. Large, dense objects are currently scanned using conventional linear accelerators that are limited in resolution because of the mm-scale source size [9]. EPAC will offer deep penetration with high temporal and spatial resolution and the potential for rapid 3D scanning. While EPAC is under construction, the CLF is continuing to work with academic and industrial partners to demonstrate the potential of laser-driven sources for practical applications using our existing lasers.

Here we report a demonstration of industrial non-destructive inspection (NDI) using high-energy (~MeV) bremsstrahlung radiation produced through conversion of an electron beam accelerated with Gemini. The experiment was a collaboration with Rolls-Royce who have an interest in dynamic NDI of aerospace components. Rolls-Royce are developing high power density electric motors and used this opportunity to bring a large rotor that has been used on a demonstrator project. NDI is needed because disassembly of the part for inspection can disturb the underlying structure. The internal features are difficult to observe with conventional imaging but should be visible with the superior resolution offered by EPAC. This particular component had a spacer ring between the magnet material and the end of the rotor, which provided good contrast to judge the success of the imaging demonstration.

This type of proof-of-principle experiment is essential. It allows testing of different operational regimes and x-ray detectors thus facilitating optimisation of image quality. Furthermore, partnerships with industry supporting development of techniques for practical applications of this capability are vital in readiness for EPAC. This brings valuable industrial expertise and product information suitable for this new x-ray technology into the EPAC project from the early stages.

Experimental method

The experiment used the full power South beam from Gemini in Target Area 3 to generate high energy (~GeV) electron bunches that impacted a metal convertor to produce bremsstrahlung x-rays. The rotor was placed on a motorised translation stage to enable movement relative to the x-ray beam. We decided that tomography was unfeasible on the timescale of this experiment and so concentrated on investigating the image quality and resolution limits by looking at features at the end of the rotor.

Equipment and configuration

A simplified schematic of the experiment is shown in Figure **1**. The laser was focussed into a plume from a high-pressure gas jet target to produce a plasma. The high electromagnetic fields generated within the plasma accelerate electrons to high energies (hundreds of MeV to GeV) in a very short distance via laser wakefield acceleration [10]. These accelerated electrons are directed onto a converter material such as iron, or tantalum, to generate bremsstrahlung radiation from the electrons [11].

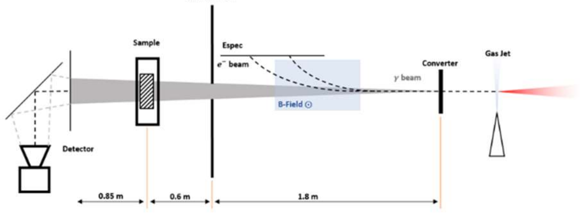

Figure 1: Schematic showing simplified layout of experiment laser (red), x-rays (grey), electrons (dashed line).

A polyimide tape drive (not shown in Figure **1**) was positioned between the gas jet target and the converter to block any laser beam that passed through the gas jet, thus avoiding damage downstream. The tape drive allows for a continual refresh of polyimide after each shot. Electrons that passed through the converter were deflected by a magnet towards an array of Lanex scintillator diagnostics observed by cameras (Espec spectrometer). The x-rays exited the vacuum chamber through a polyimide window and passed through the sample (rotor) onto a LYSO scintillator (detector head) observed by a camera (the detector) shown in Figure **2**. The detector system utilised two iXon 888 cameras with wide field of view, high sensitivity and high speed. Both cameras have a 1024 x 1024 pixel grid, with 13 µm pixel size. The low resolution detector was fitted with a DO-5095 50 mm lens with manual focus and iris having a 0.95 f-stop imaging the scintillator (the detector head). Selection of the thickness and type of scintillator used was determined as part of the characterisation and optimisation stage of the experiment.

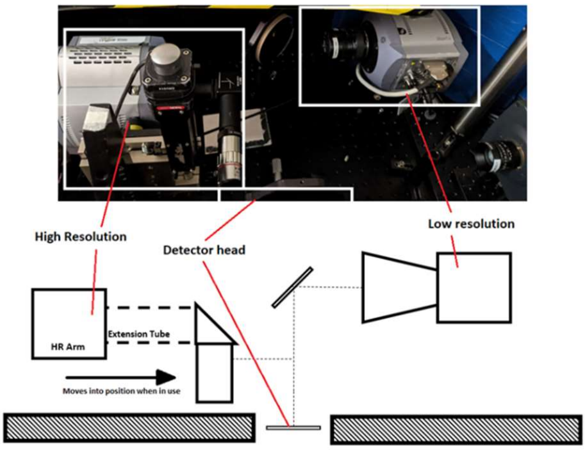

Figure 2: Photograph and illustration of detector set up.

The Rolls-Royce rotor was constructed of several radial layers around a hollow titanium shaft, as shown in Figure **3**. The rotor was mounted securely on an adjustable stage to allow remote manipulation of the sample (Figure **4**). When imaging, the sample could be adjusted horizontally along the axial direction to image the upper surface.

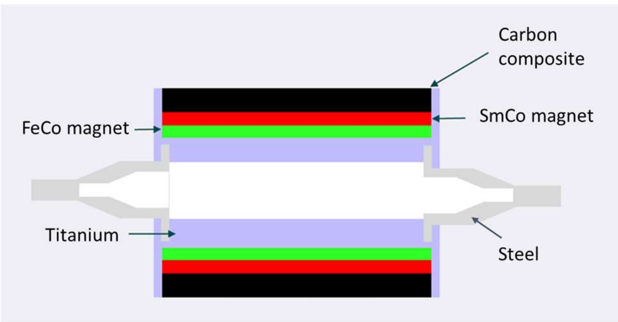

Figure 3: Schematic of the construction of the rotor supplied by Rolls-Royce.

X-ray beam characterisation and optimization

During the characterisation stage, the beam was seen to be inconsistent, with some shots producing no usable data, some producing a dim beam and others producing a bright enough image of the beam (Figure **5**). In light of this, significant optimisation effort was undertaken. As a consequence, the majority of shots taken produced usable data. Ultimately the fraction of shots producing usable data was 79.8%.
Several thicknesses of iron and tantalum were tested as convertors to optimise the beam as far as practicable. The thickest tantalum, 4.0 mm thick, was used for the experiment because it produced the best combination of x-ray flux and divergence.

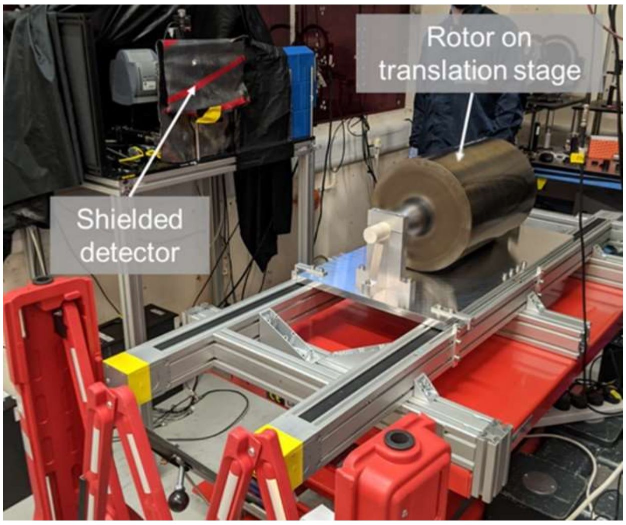

Figure 4: Photograph showing the rotor on a translation stage and the shielded x-ray detector.

The choice of scintillator was driven by the trade-off between resolution and sensitivity. Thicker scintillators provide more signal because of their greater x-ray stopping power, but this is at a cost of resolution. We investigated several thicknesses and types of scintillator (Table **1**) and found that to achieve sufficient signal level required the thickest 10mm LYSO scintillator (90 mm diameter). This limited the resolution to ~400 micron. Therefore, only the low resolution arm of the dual detector was used, because the high resolution arm would not offer any increase in resolution.

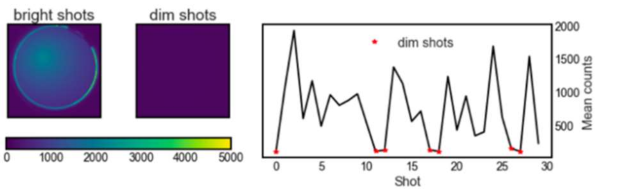

Figure 5: Beam spot characterisation: initially x-ray flux was inconsistent, but this was improved through optimisation of the system.

Scintillator	**FOV [mm]**	**Resolution estimate [micron]**	**Energy sensitivity [keV]**
LYSO 20 x 20 x 0.05 mm	2 – 5	< 20	< 100
LANEX 200 x 200 x 0.1 mm	100	100	< 250
LYSO 50 x 50 x 0.5 mm	50	50 – 100	< 250
LYSO 50 x 50 x 2 mm	50	100 – 300	< 1000
LYSO φ90 mm x 10 mm	90	200 – 800	> 1000

Table 1: Parameters of available scintillators. The best images were obtained with 10mm thick LYSO.

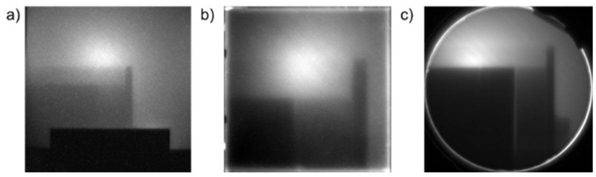

Figure 6: Single-shot imaging using (a) Lanex; (b) 2mm thick LYSO; (c) 10 mm thick LYSO. Thinner scintillators offer better resolution, but with poorer signal and contrast levels. A filter has been applied to remove hot pixels caused by hard x-ray hits.

Results

Figure **7**(a) displays the thinner section at the end of the rotor and has been averaged over several shots to improve the image quality. The bolts and threading around this region can be clearly distinguished.

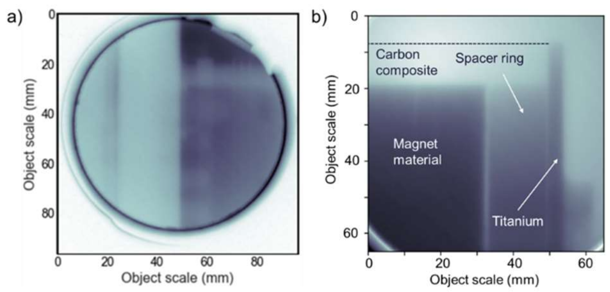

Figure 7: Images obtained averaging several shots: (a) a section of the supporting shaft with bolts and threading visible; (b) the end of the rotor showing the spacer ring between the magnet material and the titanium end plate. The carbon composite is transparent to the high energy x-rays used here.

The image in Figure **7**(b) shows the end of the rotor with good contrast. The magnet material, spacer ring, and end plate are all clearly distinguished because of their variation in attenuation. A study of known features in the rotor indicated that the image has a 400 micron resolution. Because the resolution is detector-limited, it should be possible to improve in future experiments. At the x-ray energy used here, the carbon composite is transparent. One of the key advantages of a fully developed laser-driven source is that it will be straightforward to create x-rays in different spectral ranges. Therefore, features in low Z materials such as carbon composites can be imaged as well as the thick high-density regions without moving the sample. Furthermore, in principle this could be achievable while the motor is fully operational.

Conclusions

Key features of the Rolls-Royce rotor were successfully imaged using laser-driven x-rays produced in Target Area 3. Because of limited x-ray flux, we needed to use a thick scintillator to achieve the necessary signal and contrast levels, and this set a limit on the resolution. Future experiments can concentrate on increasing the flux and tuning the energy to optimise contrast of specific samples. Higher charge beams at lower energy (1 – 30 MeV) are needed to produce the 1 – 10 MeV range x-ray photons that are more suited for radiography applications [12]. Higher flux will enable the use of thin scintillators and thus improve resolution.

While this experiment demonstrated the ability to produce useful images of relatively large and dense metal samples, Gemini has some inherent limitations that hamper progress: low shot rate, source instability, a lack of propagation distance in the target area, as well as limited opportunities for access. These issues will be addressed with EPAC, which will allow intense development and optimisation of secondary sources based on laser wakefield acceleration. This will enable advanced industrial imaging, meeting the challenges of cutting-edge product development by providing fast scanning with high temporal and spatial resolution over a wide range of x-ray energies.

References

[1] J. M. Cole et al., *Laser-Wakefield Accelerators as Hard x-Ray Sources for 3D Medical Imaging of Human Bone*, Scientific Reports **5**, 1 (2015).

[2] J. M. Cole et al., *High-Resolution µCT of a Mouse Embryo Using a Compact Laser-Driven X-Ray Betatron Source*, Proceedings of the National Academy of Sciences **115**, 6335 (2018).

[3] A. E. Hussein et al., *Laser-Wakefield Accelerators for High-Resolution X-Ray Imaging of Complex Microstructures*, Sci Rep **9**, 1 (2019).

[4] J. N. Gruse et al., *Application of Compact Laser-Driven Accelerator X-Ray Sources for Industrial Imaging*, Nuclear Instruments and Methods in Physics Research, Section A: Accelerators, Spectrometers, Detectors and Associated Equipment **983**, 164369 (2020).

[5] P. Mason et al., *Commissioning of a KW-Class Nanosecond Pulsed DPSSL Operating at 105 J, 10 Hz*, in *High-Power, High-Energy, and High-Intensity Laser Technology III*, Vol. 10238 (SPIE, 2017), pp. 36–45.

[6] P. Mason et al., *Development of a 100 J, 10 Hz Laser for Compression Experiments at the High Energy Density Instrument at the European XFEL*, High Power Laser Science and Engineering **6**, e65 (2018).

[7] M. J. V. Streeter et al., *Laser Wakefield Accelerator Modelling with Variational Neural Networks*, High Power Laser Science and Engineering **11**, e9 (2023).

[8] B. Hornberger, J. Kasahara, R. Ruth, R. Loewen, and J. Khaydarov, *Inverse Compton Scattering X-Ray Source for Research, Industry and Medical Applications*, in *International Conference on X-Ray Lasers 2020*, Vol. 11886 (SPIE, 2021), pp. 51–60.

[9] W. Sun, D. R. Symes, C. M. Brenner, M. Böhnel, S. Brown, M. N. Mavrogordato, I. Sinclair, and M. Salamon, *Review of High Energy X-Ray Computed Tomography for Non-Destructive Dimensional Metrology of Large Metallic Advanced Manufactured Components*, Rep. Prog. Phys. **85**, 016102 (2022).

[10] F. Albert and A. G. R. Thomas, *Applications of Laser Wakefield Accelerator-Based Light Sources*, Plasma Physics and Controlled Fusion **58**, (2016).

[11] C. I. D. Underwood et al., *Development of Control Mechanisms for a Laser Wakefield Accelerator-Driven Bremsstrahlung x-Ray Source for Advanced Radiographic Imaging*, (2020).

[12] A. Döpp et al., *A Bremsstrahlung Gamma-Ray Source Based on Stable Ionization Injection of Electrons into a Laser Wakefield Accelerator*, Nuclear Instruments and Methods in Physics Research Section A: Accelerators, Spectrometers, Detectors and Associated Equipment **830**, 515 (2016).